# Electrical activation in silicon-on-insulator after low energy boron implantation

Antonio F. Saavedra and Kevin S. Jones
*SWAMP Center, Department of Materials Science and Engineering, University of Florida, Gainesville, Florida 32611*

Mark E. Law
*SWAMP Center, Department of Electrical and Computer Engineering, University of Florida, Gainesville, Florida 32611*

Kevin K. Chan
*IBM Semiconductor Research and Development Center, Research Division, Yorktown Heights, New York 10598*

Erin C. Jones
*Department of Electrical and Computer Engineering, Oregon State University, Corvallis, Oregon 97331*

(Received 15 December 2003; accepted 18 May 2004)

We have investigated the electrical activation of implanted boron in silicon-on-insulator (SOI) material using Hall effect, four-point probe, and secondary ion mass spectrometry. Boron was implanted at energies ranging from 1 keV to 6.5 keV with a dose of $3\times10^{14}$ cm$^{-2}$ into bonded SOI wafers with surface silicon thickness ranging from 300 Å to 1600 Å. In one sample set, furnace anneals at 750 °C were performed in a nitrogen ambient for times ranging from 5 min to 48 h. A second sample consisted of isochronal furnace anneals performed from 450 °C to 1050 °C for 30 min. Significantly less activation of boron is observed in SOI at temperatures below 750 °C, regardless of the implant energy and surface silicon thickness. Between 750 °C and 900 °C, the active dose of boron in SOI is similar to that of bulk Si. As the implant energy increases, the fractional activation in thin SOI increases, due to a reduction in boron interstitial clusters (BIC) in the surface Si layer. It is concluded that an increase in the BIC population is the likely source of the low activation observed in SOI. This may be due to an increase in the interstitial supersaturation within the surface Si layer, due to the interface acting as a reflective boundary for interstitials. © *2004 American Institute of Physics*. [DOI: 10.1063/1.1769095]

## I. INTRODUCTION

Silicon-on-insulator (SOI) appears slated to be the replacement for bulk silicon as complementary metal-oxide-semiconductor (CMOS) devices approach the 50–60 nm technology node.[1] This is a result of the performance and fabrication advantages SOI provides.[2–5] These include increased speed, reduced power consumption, reduced short channel effects, and elimination of latchup, just to name a few. Double-gate SOI structures such as the FinFET,[6] PAGODA,[7] gate-all-around,[8] and DELTA,[9] each show promise over the traditional planar CMOS process. However, models for predicting dopant diffusion and activation in SOI are fairly limited at present.[10] Physically based models will be essential for design and fabrication of future SOI devices.

One of the challenges facing SOI model development is the presence of two interfaces. These include the traditional native oxide/silicon and surface silicon/buried oxide (BOX) interface. This results in anomalous doping profiles for both *n*-and *p*-type dopants.[11–17] As the surface silicon layer is thinned, boron tends to pileup at the surface Si/BOX interface, while phosphorus and arsenic tend to deplete.[11] For thick surface Si films and shallow implants, dopant diffusion appears similar to bulk Si.[11,18] However, the effect of dopant segregation in SOI on electrical activation has yet to be thoroughly investigated and will be critical to scaling SOI devices into the fully depleted regime.

Formation of boron interstitial clusters (BICs) is a major problem in attempting to activate junctions. Instead of the maximum active carrier concentration being limited by solid solubility of boron, BICs form at much lower concentrations. It could be hypothesized that the segregation phenomenon might affect the degree to which certain dopants tend to cluster as they pileup or deplete at the interface. Simulations by Vuong *et al.*,[12] suggest that clustering of boron in SOI is similar to bulk Si.

Robinson *et al.* investigated electrical activation of arsenic in separation by implantation of oxygen substrates and found little difference to bulk Si.[16] Other investigations of mobility in SOI metal-oxide-semiconductor field effect transistors (MOSFETs) have found reduced electron and hole mobility due to phonon scattering as the surface Si thickness is reduced.[19–22] On the other hand, for thicker SOI films the mobility in SOI is enhanced due to volume inversion.[23,24] However, these cases for MOSFETs are quite different from that of SOI material that has not been fabricated into a device. This experiment set out to investigate the effect of surface Si thickness and dopant segregation on electrical activation of implanted boron.

 

## II. EXPERIMENT

### A. Material processing

In the experiment 200 mm, (001), *p*-type, 14–22 Ω cm UNIBOND® and Czochralski substrates were used. All the SOI substrates had a BOX thickness of 400 nm. The SOI substrates, having an initial surface Si thickness of 1600 Å, were thinned to 700 Å and 300 Å using oxidation and etching in dilute HF (10:1). Prior to ion implantation, a screen oxide was thermally grown in a wet oxygen ambient to help reduce channeling of the boron ions. Room temperature nonamorphizing ion implantation of $^{11}B^+$ at a dose of $3\times10^{14}$ cm$^{-2}$ was performed for energies ranging from 1 keV to 6.5 keV at a 7° tilt and 22° twist angle. Implant energies were designed to place the projected range of the implant at varying depths within the surface Si layer. Following the implants, a low temperature oxide (LTO) of 20 nm was deposited at 425 °C in order to prevent dopant out diffusion of the shallow implants. This was performed using a plasma enhanced chemical vapor deposition system with the screen oxide still in place. Specimens were scribed into squares ranging from 10 mm×10 mm to 14 mm×14 mm. Anneals were performed in a Lindberg quartz tube furnace in a nitrogen ambient. Isothermal anneals at 750 °C for times of 5 min to 48 h were done to activate the implanted boron. Separate isochronal anneals for 30 min at temperatures of 450–1050 °C was also performed to understand the temperature dependence of the activation process.

### B. Analytical techniques

Hall effect was performed using an MMR Technologies system with a MPS-50 programmable power supply and H-50 Hall, van der Pauw field controller. A magnetic field of 3000 G was used in all of the measurements. Current was varied from $1\times10^{-7}$ A to $1\times10^{-3}$ A in order to check the linearity of the Hall measurements. This allowed measurement of the hole mobility, sheet number, and sheet resistance. Hall scattering factors were determined by annealing specimens at 1000 °C for 2 h to obtain complete activation of the specimens. The active dose obtained was then divided by the implanted dose to yield the scattering factor. These were approximately 0.9, 0.9, 0.7, and 0.85, for the 300 Å, 700 Å, 1600 Å, and bulk, respectively.

Four-point probe measurements were done using a Jandel multi height probe. A current of 438.02 μA was used for bulk Si and 38.02 μA for SOI. Geometrical correction factors were used since sample sizes greatly exceeded the probe spacing. Four-point probe was mainly used to compare sheet resistance values with those obtained from the Hall–van der Pauw, ensuring the reliability of the measurements.

Secondary ion mass spectrometry (SIMS) was performed using a CAMECA IMS-3F secondary ion mass spectrometer. An $O_2^+$ primary ion beam with an energy of 15 keV and 15° incident angle was used for obtaining boron concentration profiles. An ion beam current of 100 nA was used, along with an electron gun to assist with charge neutralization in the BOX. This helped to determine the amount of boron segregation towards the BOX as annealing proceeded.

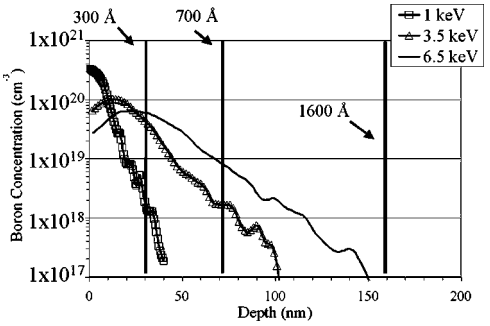


FIG. 1. UT-MARLOWE ion profile simulations for $B^+$ implants at 1 keV, 3.5 keV, 6.5 keV, $3\times10^{14}$ cm$^{-2}$. Note location of surface Si/BOX interface for 300 Å, 700 Å, and 1600 Å SOI.

## III. RESULTS

UT-MARLOWE[25] simulations were used to determine the amount of as-implanted dose loss to the BOX. This was done, in the case of SOI, by truncating the ion/boron concentration profile at the surface Si/BOX interface and integrating the portion of the profile remaining in the surface Si layer. Figure 1 shows the ion concentration profiles obtained using UT-MARLOWE, while Fig. 2 shows percent dose retained calculated from the simulations. This is important to keep track of, since boron can certainly not serve as an acceptor if it lies in the BOX. Thus, it would affect the electrical measurements obtained from Hall and four-point probe. All the implant energies resulted in dose loss in the 300 Å SOI, ranging from less than 1% at 1 keV to 50% at 6.5 keV. The 700 Å SOI lost 6% of the dose at 6.5 keV, but did not lose any for the 1 keV or 3.5 keV. No dose loss to the BOX occurred in the 1600 Å SOI for any of the implants simulated.

Electrical data obtained from Hall effect measurements for the 1 keV and 6.5 keV implant energies annealed at 750 °C are shown in Figs. 3 and 4, respectively. Significantly less activation [Figs. 3(a) and 4(a)] can be seen to occur in all of the SOI specimens compared to bulk Si. Even after annealing for 48 h, the active dose in SOI does not approach that of bulk Si. The hole mobility ($\mu_h$) and sheet resistance ($R_s$) are also lower in SOI by roughly 300 cm$^2$/V s. The sheet resistance in the 1600 Å SOI appears to be slightly less than the 700 Å and 300 Å. The bulk

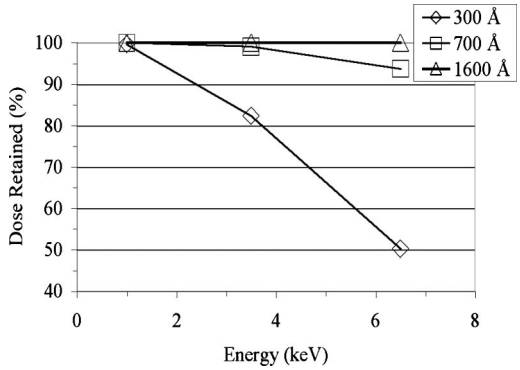


FIG. 2. Percent retained dose of boron in surface Si layer as function of implant energy for 300 Å, 700 Å, and 1600 Å SOI. Calculated using UT-MARLOWE ion profiles.

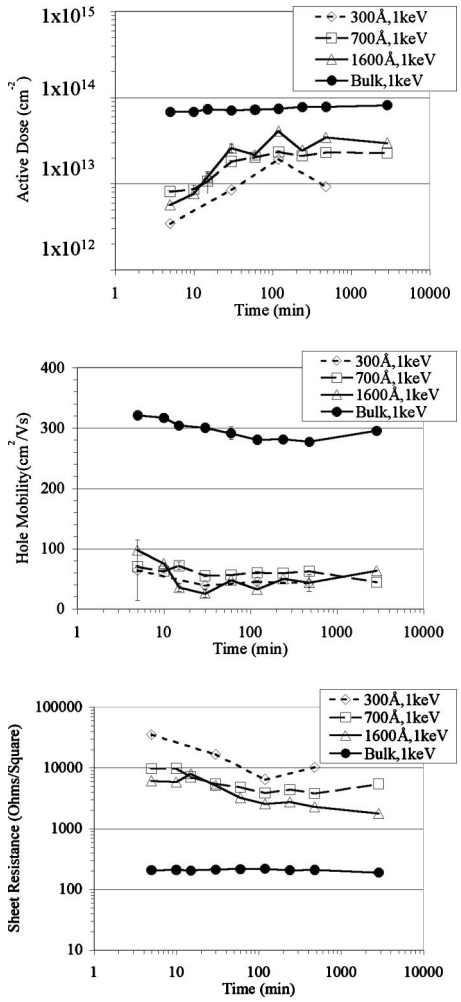


FIG. 3. Isothermal Hall data for $B^+$, 1 keV, $3\times10^{14}$ cm$^{-2}$ at 750 °C including (a) active dose, (b) hole mobility, and (c) sheet resistance.

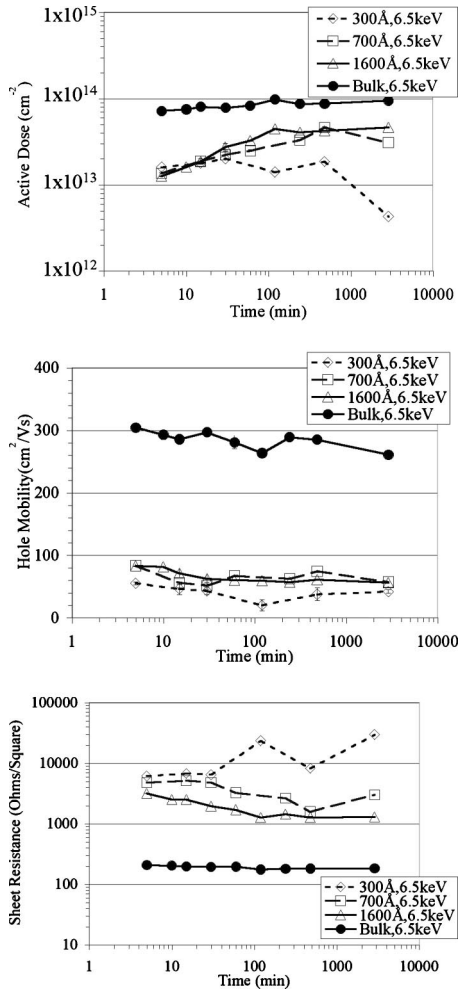


FIG. 4. Isothermal Hall data for $B^+$, 6.5 keV, $3\times10^{14}$ cm$^{-2}$ at 750 °C including (a) active dose, (b) hole mobility, and (c) sheet resistance.

Si results compare favorably with those of Ref. 26, in terms of active dose, for boron implants at similar energies and doses. However, when compared to mobilities obtained by Ref. 27 the problem appears to be that the bulk Si has an enhanced mobility rather than SOI being degraded. Sasaki *et al.*, found mobilities for boron concentrations between $1\times10^{19}$ cm$^{-3}$ and $1\times10^{20}$ cm$^{-3}$ to be between 70 and 53 cm$^2$/V s, respectively.[27] Figure 5 compares the sheet resistance obtained from four-point probe with Hall effect for each of the implant energies. The $R_s$ values agree well, indicating the measurements are indeed reliable and not a result of instrument error.

Figures 6 and 7 show the isochronal Hall effect data for the 1 keV and 6.5 keV implant energies, respectively. For the 1 keV SOI specimens, the active dose was over two orders of magnitude less compared to bulk Si for temperatures less than 600 °C. Significant activation occurs between 600 °C and 750 C in SOI. The 700 Å and 1600 Å activate slightly more than bulk si as the annealing temperature exceeded 900 °C. Once again, lower mobility and sheet resistance occur in SOI, but the mobility is close to that found in Ref. 27. A significant decrease in mobility occurs in SOI and bulk Si as the temperature increases. This is attributed to ionized impurity scattering as more boron atoms begin to occupy Si lattice sites.[28] The sheet resistance in SOI does begin to approach bulk Si as the annealing temperature increases. For the 300 Å SOI implanted at 6.5 keV, the active dose is higher below 600 °C than the 700 Å and 1600 Å. This is surprising considering the increase in dose loss in the 300 Å SOI; intuitively, one would expect less dose to result in a lower active dose since carriers cannot activate in an oxide. However, it is likely due to a reduction in the BIC population for the 300 Å SOI. This is discussed further in the Discussion.

SIMS profiles for the 300 Å SOI annealed at 750 °C are shown in Fig. 8. Segregation of boron into the BOX occurs after annealing for 30 min, indicated by the depletion of boron as the surface Si/BOX interface is approached. Most segregation appears to take place in the first 30 min at 750 °C, as evidenced by the 120 min profile.

## IV. DISCUSSION

The data acquired show that a significant difference exists in the activation process between SOI and bulk. Activation in bulk Si shows a diminished temperature dependence compared to SOI. However, it is difficult to directly compare the two because of the higher activation in bulk Si at low thermal budgets. This indicates that significant activation in

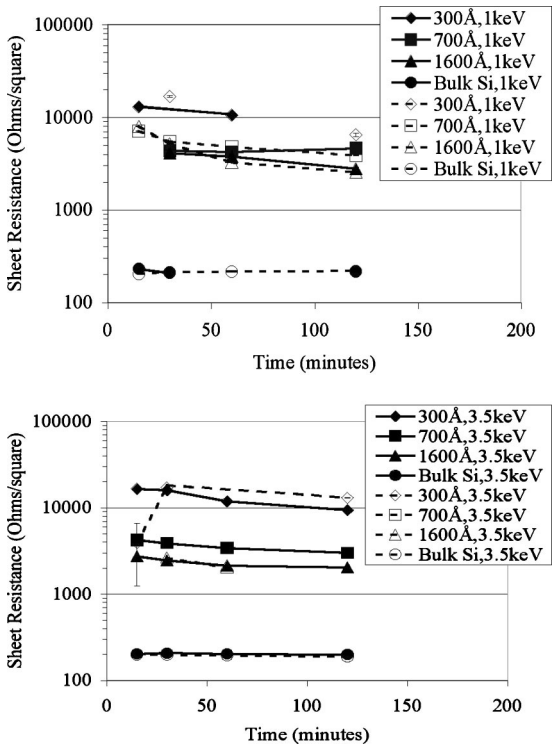


FIG. 5. Comparison of sheet resistance data measured by four-point probe and Hall effect for (a) 1 keV, (b) 3.5 keV, and (c) 6.5 keV, $3\times10^{14}$ cm$^{-2}$ annealed at 750 °C. Solid symbols and lines represent four-point probe measurements and open symbols represent Hall measurements.

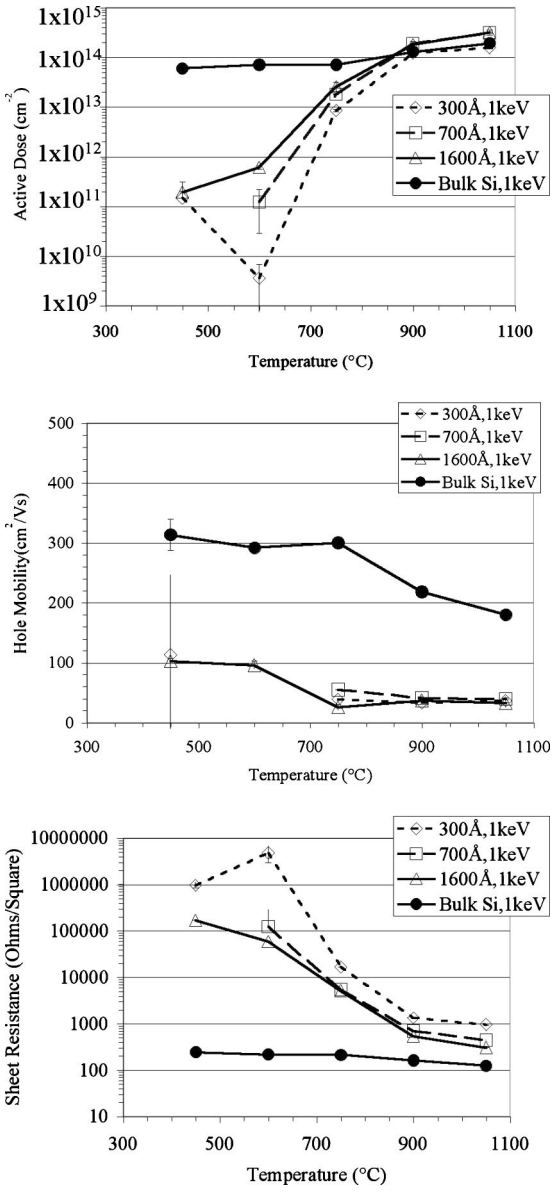


FIG. 6. Isochronal Hall data for $B^+$, 1 keV, $3\times10^{14}$ cm$^{-2}$ after annealing for 30 min showing (a) active dose, (b) hole mobility, and (c) sheet resistance.

bulk Si may have occurred during the LTO deposition. The boron implants were nonamorphizing, so solid phase epitaxy did not occur in the experiments. This may have explained the higher activation in bulk Si at low temperatures, but this was not the case. Significant transient enhanced diffusion (TED) was observed in the bulk Si SIMS profiles. This eliminates the possibility of other thermal processing accidentally taking place that could have activated the boron in bulk Si. This may have been a valid point if no TED was observed, but this was also not the case. It could also be speculated that the results are simply an artifact of performing Hall effect on thin Si films. If this was the case full activation would not have been obtained, yet the results in Figs. 6 and 7 show that 100% activation was obtained in thick SOI annealed at high temperatures. The effects of boron clustering, segregation, impurity trapping, and thermal strain on the electrical activation results presented above are each discussed separately.

### A. Boron interstitial clusters

As indicated previously, high concentrations of boron in the presence of an interstitial supersaturation can result in the formation of boron-interstitial clusters (BICs).[29] This is generally accepted to occur between $1\times10^{18}$ cm$^{-3}$ and $1\times10^{19}$ cm$^{-3}$ boron concentrations.[29–32] Clustering is often observed as immobile peaks in SIMS profiles, low Hall doses, as well as reductions in the trapped interstitial population in extended defects.[33] The boron concentrations in the present study are well above the clustering limit according to Fig. 8. Thus, it could be proposed that the lack of activation is a result of an increase in BICs in SOI. If more of the boron binds with the excess interstitials, it could reduce the electrical activation, assuming that particular BIC complex is not electrically active. Also, if a higher interstitial supersaturation is present in the surface Si layer it could provide the extra interstitials to allow for the increase in BIC population.[34]

It has been shown that a reduction in the trapped interstitial dose in {311} defects occurs in SOI after boron implantation at 6.5 keV and 19 keV, $3\times10^{14}$ cm$^{-2}$.[35] The authors attributed this to an increase in BIC formation in SOI. However, the microstructure consists mainly of small dot defect clusters at 1 keV and 3.5 keV, rather than larger extended defects such as {311}s and dislocation loops. The dot defects are more difficult to accurately quantify due to their small size, thus there could be significant error in the QTEM measurements at the lowest energies. This would tend to support the BIC theory in thick SOI.

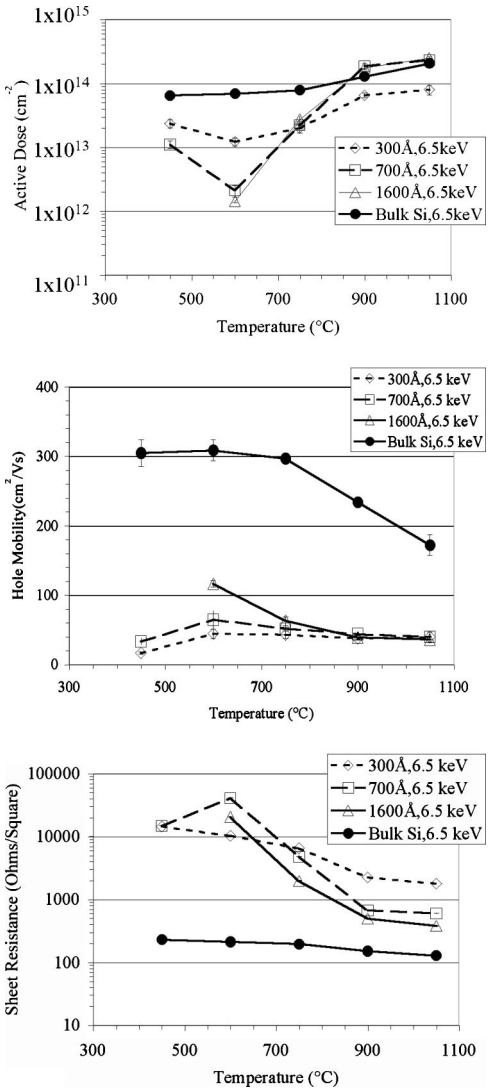


FIG. 7. Isochronal Hall data for $B^+$, 6.5 keV, $3\times10^{14}$ cm$^{-2}$ after annealing for 30 min showing (a) active dose, (b) hole mobility, and (c) sheet resistance.

A theory could be proposed suggesting that perhaps the surface Si/BOX interface actually prevents interstitials from diffusing into or recombining at the BOX. Rather, the interface tends to behave as a more reflective boundary for interstitials. Interstitials released from the extended defects would tend to remain within the surface Si layer and be available to

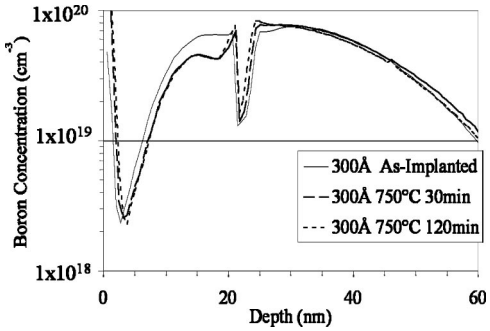


FIG. 8. Boron concentration profiles from SIMS for 300 Å SOI implanted at 6.5 keV, $3\times10^{14}$ cm$^{-2}$ then annealed at 750 °C. Note segregation of boron into buried oxide.

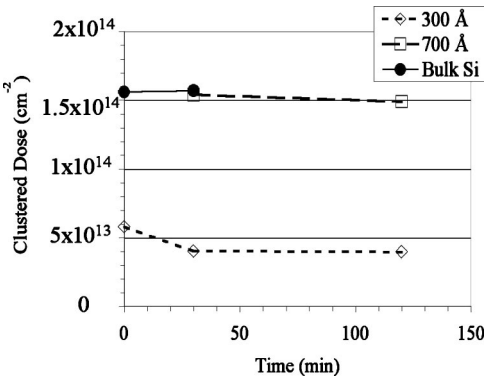


FIG. 9. Clustered dose in SOI and bulk Si for $B^+$, 6.5 keV, $3\times10^{14}$ cm$^{-2}$ annealed at 750 °C. Dose was obtained by integrating the B concentration profiles that lie above a level of $1\times10^{19}$ cm$^{-3}$.

participate in the BIC process. This would explain the low activation observed for SOI. This theory would not be out of the realm of possibility based on results from previous experiments that show the interface is a weak sink for interstitials unless a large amount of the dose is lost to the BOX during the implant.[35–38] It has also been conjectured that the contact potential at the $Si/SiO_2$ interface sets up an electric field that is likely to repel interstitials for *p*-type material.[39]

A BIC theory also explains why the 300 Å SOI activated more than the thicker SOI at low temperatures for the 6.5 keV implant. Figure 9 shows the clustered dose in SOI and bulk Si for the 6.5 keV annealed at 750 °C. The clustered dose was obtained by subtracting $1\times10^{19}$ cm$^{-3}$ from the boron concentration in the SIMS profiles and then integrating over the surface Si thickness. The significant reduction in clustered dose for the 300 Å SOI explains the higher activation that was measured despite the dose loss of boron to the BOX. This is due to an immediate loss of interstitials to the BOX due to the implant energy. The influence of a shallow vacancy rich region near the surface could also become more critical as interstitial loss to the BOX occurs. MeV energy $Si^+$ implants have been used previously to provide a vacancy rich region closer to the surface. This, in conjunction with boron implantation near the peak of the vacancy profile, allows for *I-V* recombination to occur and thus reduce BIC formation.[40] However, the influence of a vacancy rich region produced by low keV implants without the aid of the MeV $Si^+$ implantation has not been experimentally observed to affect clustering. Figure 10 shows the fraction of active boron and has been adjusted to account for the dose loss in thin SOI. The fractional active dose was computed by dividing the active dose measured from Hall by the total retained dose within the surface Si layer. It illustrates that the 300 Å SOI is able to approach bulk Si in terms of fractional activation at low temperatures. This further supports that interstitials are being lost to the BOX in thin SOI, thus reducing the BIC population. The dose loss argument explains why the active dose does not approach that of the thick SOI at higher temperatures.

### B. Boron segregation

Another theory that could be proposed to explain the lack of activation in SOI is that of boron segregation to the

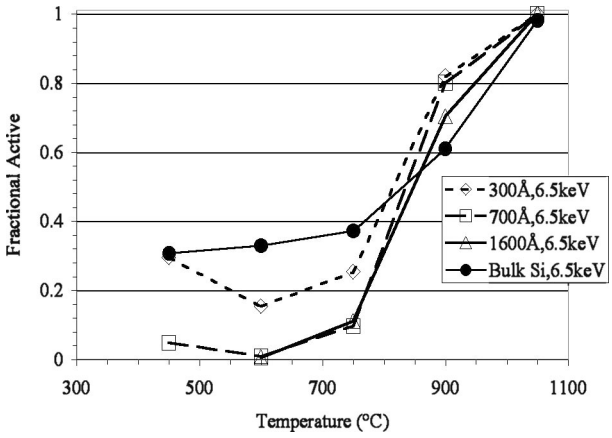


FIG. 10. Active fraction of boron in SOI and bulk for 6.5 keV, $3\times10^{14}$ cm$^{-2}$ annealed for 30 min.

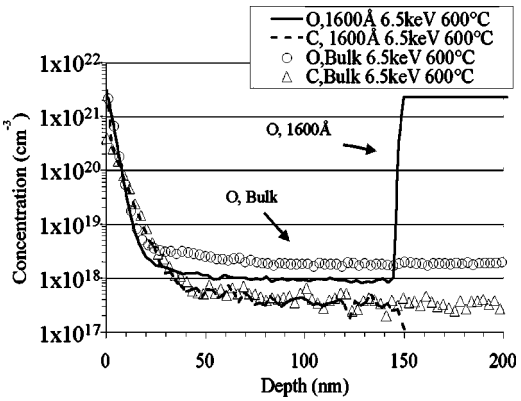


FIG. 11. Carbon and oxygen SIMS profiles for 1600 Å SOI and bulk Si implanted with $B^+$, 6.5 keV, $3\times10^{14}$ cm$^{-2}$, and annealed at 600 °C for 30 min.

BOX. Significant segregation could result in dose loss to the BOX that would prevent the boron from activating. It is also not known whether boron pileup at the surface Si/BOX interface is active or not. The theory of dose loss can be disproved by realizing the amount of boron that would be required to segregate to the BOX in thick SOI. Significant segregation/dose loss does not occur in the 1600 Å SOI at the energies studied, so it cannot explain the low activation. Rather, the segregation is limited by the segregation coefficient (~0.3 for B) (Ref. 41) for boron in the two materials. Once the chemical potential between the two materials is equilibrated the boron ceases to segregate. The issue of pileup in thin SOI can be addressed by comparing the active dose obtained from Hall to the integrated SIMS dose remaining in the surface Si layer. This results in an active fraction of boron in the 300 Å SOI of 0.2–0.25, while the 1600 Å is closer to 0.1–0.13 (see Fig. 10). This indicates that the segregation in thin SOI does not result in significant deactivation of the boron. Rather, as indicated above, the reduction in BIC population promotes the activation of the boron in thin SOI.

### C. Impurity trapping

A third theory might involve contaminants, such as C and O, serving as traps for the interstitials.[42] If this was the case the C and O could trap the interstitials present in the extended defects.[43,44] This could explain the QTEM data from our previous work.[35] However, it does not explain the QTEM data performed for $Si^+$ implants into SOI where no significant difference was observed for implant profiles confined to the surface Si layer.[36] This indicates that the presence of boron is the major source of the reduction in trapped interstitials in Ref. 35. Figure 11 shows C and O SIMS profiles obtained for SOI and bulk Si. The carbon levels for SOI and bulk are similar, while slightly more oxygen exists in bulk Si. This difference does not affect the trapping efficiency of extended defects in the bulk, though.

### D. Thermal strain

One final theory could be developed based on thermal strain present in SOI. This is due to differences in the linear thermal expansion coefficient between silicon and silicon dioxide, as well as the BOX and surface Si thickness. These values are $2.6\times10^{-6}$ °C$^{-1}$ and $5\times10^{-7}$ °C$^{-1}$ for silicon and silicon dioxide, respectively.[45] Compressive stresses have been shown to significantly affect dopant diffusion in Si depending on their magnitude.[46–48] Enhancements of 2× in the diffusivity of boron have been observed for pressures approaching 5 GPa.[43] Unfortunately, there have not been many studies to understand the effect of stress on activation in Si. It could be proposed that as SOI is annealed the strain in the surface Si layer increases due to the mismatch, thus preventing the boron from occupying substitutional lattice sites. However, above a certain temperature the BOX begins to viscously flow[49] and accommodate the strain in the surface Si layer. The process of viscous flow of $SiO_2$ typically occurs around 1000 °C, but this can be reduced depending on whether or not the $SiO_2$ is hydrated. This would allow the boron to occupy substitutional sites in the lattice and increase the activation in SOI. This theory could explain the lack of activation in SOI at low temperatures, as well as the activation at higher temperatures.

For tensile thermal stresses, the linear expansion coefficient is related to the change in elongation per unit temperature according to

$$\alpha = \frac{\Delta l}{l_0(T - T_0)}, \tag{1}$$

where $\alpha$ is the linear thermal expansion coefficient, $\Delta l$ is the change in elongation, $l_0$ is the original length, and $\Delta T$ is the change in temperature in Kelvin. The tensile strain is given as

$$\varepsilon = \frac{\Delta l}{l_0} = \alpha(T - T_0), \tag{2}$$

where $\varepsilon$ is the engineering strain. Using Hooke's Law, the thermal stress is

$$\alpha = E\varepsilon = E\alpha(T - T_0), \tag{3}$$

where $\sigma$ is stress. Stoney[50] developed a method, based on the mechanics of beam bending, by which the stress in thin films on substrates may be calculated. Stoney's formula is commonly stated as

$$\alpha_f = \frac{F_f}{d_f w} = \frac{1}{6R}\frac{E_s d_s^2}{(1-\upsilon_s)d_f}, \tag{4}$$

where $\sigma_f$ is the film stress, $F_f$ the force exerted by the thin film, $d_f$ the film thickness, $w$ the width of the film, $R$ the radius of curvature of the film, $E_s$ the elastic modulus of the substrate material, $d_s$ the substrate thickness, and $\upsilon_s$ Poisson's ratio of the substrate.[51] Combining the effects of thermal strain and mechanical strain the total strain in the film and substrate are given as

$$\varepsilon_f = \alpha_f \Delta T + \frac{F_f(1-\upsilon_f)}{E_f d_f w}, \tag{5}$$

$$\varepsilon_s = \alpha_s \Delta T - \frac{F_f(1-\upsilon_s)}{E_s d_s w}. \tag{6}$$

In order for mechanical equilibrium to hold, $\varepsilon_f$ must be equal to $\varepsilon_s$. This allows for calculation of the thermal mismatch force $F_f$ by manipulating Eqs. (5) and (6). Since $d_s \gg d_f$, for case involving partially depleted SOI and fully depleted SOI, the film stress due to thermal mismatch between a film and its substrate can be stated as

$$\alpha_f(T) = \frac{F_f}{d_f w} = \frac{(\alpha_s - \alpha_f)\Delta T E_f}{(1-\upsilon_f)}. \tag{7}$$

SOI can be thought of as a multilayer structure consisting of two thin films on a bulk Si substrate. During annealing, the Si substrate expands at a greater rate than the BOX, thus creating a tensile stress in the overlying BOX. As SOI is allowed to cool down, the substrate also contracts at a greater rate than the BOX, allowing for a residual compressive stress to form in the layers. The intrinsic compressive stress in thermally grown $SiO_2$ has been measured to be between −0.2 GPa and −0.3 GPa, which is close to that predicted by Eq. (7) assuming viscous flow above 1000 °C.[52] According to Hooke's Law, this would correspond to a strain of 0.25%–0.38% in the BOX. However, this stress would tend to be reduced during annealing since the films would expand/contract oppositely from that occurring during cool down. This pressure would not be significantly high enough to enhance the diffusivity of B in Si according to Zhao *et al.*,[46] thus tending to shed doubt on this theory. SIMS profiles on the thick SOI and bulk Si confirmed that this was the case, as the diffusivity within the tail of the profiles appeared similar.

## V. CONCLUSIONS

We have investigated the process of electrical activation of boron in SOI scaled to 300 Å using Hall effect, four-point probe, and SIMS. We show a significant decrease in the active dose of boron in SOI compared to bulk Si at low annealing temperatures. Lower mobility and increased sheet resistance are also observed, but the mobility in SOI is close to that observed previously. Above approximately 900 °C the boron active dose in SOI approaches that of bulk Si. All these effects appear regardless of the surface Si thickness and implant energy. It is also shown that as the implant energy increases, fractional activation in thin SOI increases, likely due to a reduction in boron interstitial clusters in the surface Si layer. A number of theories are proposed to explain the lack of activation in SOI, but boron interstitial clustering appears the most likely source. These results could have significant impact on low temperature processes in SOI such as solid phase epitaxy, as well as high temperature annealing using high ramp rates. Future work will involve an in depth high-resolution x-ray diffraction study to determine the precise role of strain in thermal processing of SOI.

## ACKNOWLEDGMENTS

The efforts of the Advanced Si Technology Laboratory at the IBM T.J. Watson Research Center are greatly appreciated. The authors are indebted to Mikhail Klimov from the University of Central Florida for providing SIMS analysis. This work was supported by the Semiconductor Research Corporation (SRC) under task 819.001.

[1] H.-S. P. Wong, IBM J. Res. Dev. **46**, 133 (2002).
[2] G. K. Celler and S. Cristoloveanu, J. Appl. Phys. **93**, 4955 (2003).
[3] J. P. Colinge, *Silicon-on-Insulator Technology: Materials to VLSI*, 2nd ed. (Kluwer, Boston, 1997), pp. 1–4.
[4] S. Cristoloveanu and S. S. Li, *Electrical Characterization of Silicon-on-Insulator Materials and Devices*, 1st ed. (Kluwer, Boston, 1995), pp. 1–4.
[5] A. Plößl and G. Kräuter, Solid-State Electron. **44**, 775 (2000).
[6] L. Chang, Y.-K. Choi, J. Kedzierski, N. Lindert, P. Xuan, J. Bokor, C. Hu, and T.-J. King, IEEE Circuits Devices Mag. **2003**, 35.
[7] P. M. Solomon *et al.*, IEEE Circuits Devices Mag. **2003**, 48.
[8] J. P. Colinge, M. H. Gao, A. Romano, H. Maes, and C. Claeys, Tech. Dig. - Int. Electron Devices Meet. **1990**, 353.
[9] D. Hisamoto, T. Kaga, and E. Takeda, IEEE Trans. Electron Devices **38**, 1419 (1991).
[10] M. Ieong and P. Oldiges, Proceedings of International Conference on Simulation of Semiconductor Processes and Devices, 2002, p. 225.
[11] H. Park, E. C. Jones, P. Ronsheim, C. Cabral, Jr., C. D'Emic, G. M. Cohen, R. Young, and W. Rausch, Tech. Dig. - Int. Electron Devices Meet. **1999**, 337.
[12] H.-H. Vuong *et al.*, Appl. Phys. Lett. **75**, 1083 (1999).
[13] P. Normand, D. Tsoukalas, N. Guillemot, and P. Chenevier, J. Appl. Phys. **66**, 3585 (1989).
[14] A. Ogura and M. Hiroi, Thin Solid Films **397**, 56 (2001).
[15] P. Normand, D. Tsoukalas, N. Guillemot, and J. Stoemenos, J. Electrochem. Soc. **137**, 2306 (1990).
[16] A. K. Robinson, K. J. Reeson, and P. L. F. Hemment, J. Appl. Phys. **68**, 4340 (1990).
[17] S. W. Crowder, C. J. Hsieh, P. B. Griffin, and J. D. Plummer, J. Appl. Phys. **76**, 2756 (1994).
[18] O. Dokumaci *et al.*, presented at 2002 MRS Spring Meeting, Symp. C, San Francisco, CA.
[19] M. Shoji and S. Horiguchi, J. Appl. Phys. **85**, 2722 (1999).
[20] M. Mastrapasqua, D. Esseni, G. K. Celler, C. Fiegna, L. Selmi, and E. Sangiorgi, Microelectron. Eng. **59**, 409 (2001).
[21] F. Gamiz, J. A. Lopez-Villanueva, J. B. Roldan, J. E. Carceller, and P. Cartujo, IEEE Trans. Electron Devices **45**, 1122 (1998).
[22] F. Gamiz and M. V. Fischetti, J. Appl. Phys. **89**, 5478 (2001).
[23] A. Vandooren, S. Cristoloveanu, D. Flandre, and J. P. Colinge, Solid-State Electron. **45**, 1793 (2001).
[24] F. Gamiz, J. B. Roldan, J. A. Lopez-Villanueva, P. Cartujo-Cassinello, J. E. Carceller, P. Cartujo, and F. Jimenez-Molinos, Solid-State Electron. **45**, 613 (2001).
[25] UT-MARLOWE Version 5.0, University of Texas-Austin.
[26] A. D. Lilak, Ph.D. Dissertation, University of Florida, 2001.
[27] Y. Sasaki, K. Itoh, E. Inoue, S. Kishi, and T. Mitsuishi, Solid-State Electron. **31**, 5 (1988).
[28] D. K. Shroeder, *Semiconductor Material and Device Characterization*, 2nd ed. (Wiley, New York, 1998) p. 100.
[29] P. A. Stolk, H.-J. Gossmann, D. J. Eaglesham, D. C. Jacobson, C. S. Rafferty, G. H. Gilmer, M. Jariz, and J. M. Poate, J. Appl. Phys. **81**, 6031 (1997).
[30] S. Mirabella, E. Bruno, F. Prilo, D. De Salvador, E. Napolitani, A. V.

Drigo, and A. Carnera, Appl. Phys. Lett. **83**, 680 (2003).
[31]L. Radic, A. D. Lilak, and M. E. Law, Appl. Phys. Lett. **81**, 826 (2002).
[32]A. D. Lilak, M. E. Law, L. Radic, K. S. Jones, and M. Clark, Appl. Phys. Lett. **81**, 2244 (2002).
[33]J. Liu, Ph.D. Dissertation, University of Florida, 1996.
[34]G. Mannino, N. E. B. Cowern, F. Roozeboom, and J. G. M. van Berkum, Appl. Phys. Lett. **76**, 855 (2000).
[35]A. F. Saavedra, A. C. King, K. S. Jones, E. C. Jones, and K. K. Chan, J. Vac. Sci. Technol. B **22**, 459 (2004).
[36]A. F. Saavedra, J. Frazer, K. S. Jones, I. Avci, S. K. Earles, M. E. Law, and E. C. Jones, J. Vac. Sci. Technol. B **20**, 2243 (2002).
[37]A. F. Saavedra, K. S. Jones, M. E. Law, and K. K. Chan, J. Electrochem. Soc. **151**, G266 (2004).
[38]A. F. Saavedra, K. S. Jones, M. E. Law, and K. K. Chan, Mater. Sci. Eng., B **107**, 198 (2004).
[39]K. Dev, M. Y. L. Jung, R. Gunawan, R. D. Braatz, and E. G. Seebauer, Phys. Rev. B **68**, 195311 (2003).
[40]R. Kalyanaraman, V. C. Venezia, L. Pelaz, T. E. Haynes, H.-J. L. Gossmann, and C. S. Rafferty, Appl. Phys. Lett. **82**, 215 (2003).
[41]R. C. Jaegar, *Introduction to Microelectronic Fabrication*, 2nd ed. (Prentice Hall, Upper Saddle River, NJ, 2002), p. 51.
[42]P. Werner, H.-J. Gossmann, D. C. Jacobson, and U. Gösele, Appl. Phys. Lett. **73**, 2465 (1998).
[43]P. B. Griffin, S. T. Ahn, G. W. Tiller, and J. D. Plummer, Appl. Phys. Lett. **51**, 115 (1987).
[44]H. Rücker, B. Heinemann, D. Bolze, R. Kurps, D. Krüger, G. Lippert, and H. J. Osten, Appl. Phys. Lett. **74**, 3377 (1999).
[45]J. D. Plummer, M. D. Deal, and P. B. Griffin, *Silicon VLSI Technology: Fundamentals, Practice and Modeling*, 1st ed. (Prentice Hall, Upper Saddle River, NJ, 2000), pp. 788–789.
[46]Y. Zhao, M. J. Aziz, H.-J. Gossmann, S. Mitha, and D. Shiferi, Appl. Phys. Lett. **74**, 31 (1999).
[47]M. J. Aziz, Mater. Sci. Semicond. Process. **4**, 397 (2001).
[48]H. Park, K. S. Jones, J. A. Slinkman, and M. E. Law, J. Appl. Phys. **78**, 3664 (1995).
[49]Y.-M. Chiang, D. Birnie III, and W. D. Kingery, *Physical Ceramics: Principles for Ceramic Science and Engineering*, 1st ed. (Wiley, New York, 1997), p. 510.
[50]G. G. Stoney, Proc. R. Soc. London **A82**, 172 (1909).
[51]M. Ohring, *The Materials Science of Thin Films*, 1st ed. (Academic, San Diego, 1992) pp. 416–420.
[52]S. M. Hu, J. Appl. Phys. **70**, R53 (1991).